Carbon 112 (2017) 63–71

Contents lists available at ScienceDirect

Carbon

journal homepage: www.elsevier.com/locate/carbon

# Small but strong: The influence of fluorine atoms on formation and performance of graphene quantum dots using a gradient F-sacrifice strategy

Peiwei Gong [a, b], Jinqing Wang [a, *], Kaiming Hou [a], Zhigang Yang [a], Zhaofeng Wang [a], Zhe Liu [b], Xiuxun Han [a, **], Shengrong Yang [a]

[a] State Key Laboratory of Solid Lubrication, Lanzhou Institute of Chemical Physics, Chinese Academy of Sciences, Lanzhou, 730000, PR China
[b] Key Laboratory of Life-Organic Analysis of Shandong Province, Qufu Normal University, Qufu, 273165, PR China

ARTICLE INFO

*Article history:*
Received 21 July 2016
Received in revised form
28 September 2016
Accepted 29 October 2016
Available online 31 October 2016

ABSTRACT

Fluorinated graphene quantum dots (FGQDs) have distinctive charge distribution in structure and unique chemical bonds in composition, corresponding to novel performance different from common quantum dots. However, their synthesis is a challenge due to chemically inert C–F bonds and hydrophobic nature, and the fluorine influence on FGQDs remains scarce and to be studied. Herein, we first design a gradient fluorine-sacrificing strategy to synthesize FGQDs with controllable sizes and tunable fluorine contents from bulk fluorinated graphite. It is found that although fluorine atom is the second-smallest in periodic table, it not only greatly affects the size formation process, but also endows FGQDs with pH-independent luminescence without any additional surface passivation. And it is for the first time to experimentally observed that point defects in FGQDs induced by fluorine can greatly increase paramagnetism, which is 5 times higher than unfluorinated ones. Moreover, cytotoxicity experiments clearly reveal FGQDs show good biocompatibility, and it is the chemical surface rather than size that influences the cell viability. This work realizes fine control over both structure and chemistry of FGQDs, and thus allows a better insight into the fluorine effects on formation and performance of graphene quantum dots.



## 1. Introduction

Recent years have witnessed significant breakthroughs and prosperity of graphene quantum dots (GQDs) in both scientific and technological worlds due to its noble and novel properties [1–3]. With characteristic quantum-confinement and edge effects, the zero-dimensional (0D) GQDs have offered numerous possibilities and opportunities for researching the fundamental science in 0D layered structures [4,5], improving the performance via the integration of graphene into various electronic and optical applications [6,7], and promoting the revolution of traditional quantum dots in environmental and biological field [8,9]. And what makes it a more versatile and applicable material is decorating GQDs with functional groups or doping the structure with heteroatoms; chemical modification of GQDs with heteroatoms is of fundamental importance to tune their intrinsic structural properties [10], manipulate the electronic state [11], and adjust surface or local chemical environment [12], etc. Discovery or successful modification of GQDs with exotic atoms, can not only ignite tremendous fresh research interest and new insights into material science, but also induce fast explosion of novel applications of GQDs [13].

Fluorine, a small atom in period table, is powerful in modulating the chemical, structural and electronic features of carbon material owing to its high electronegativity. Decorating graphene with fluorine (namely fluorinated graphene, FG) has endowed graphene with unique electronic [14,15], luminescent [16,17], magnetic [18,19], electrochemical [20,21] and biological function [22,23], etc. And then it inspires us to deeply think what it will bring about as grafting fluorine onto GQDs. However, both the challenge of preparing FG and the dramatic inertia of C–F chemical bonds unmercifully make most of once available methods to prepare GQDs invalid. Accordingly, it remains a great challenge to prepare FGQDs, and the unique properties of FGQDs are almost completely unknown, not to mention its potential applications. Therefore, in view

* Corresponding author.
** Corresponding author.
*E-mail address:* jqwang@licp.cas.cn (J. Wang).

http://dx.doi.org/10.1016/j.carbon.2016.10.091
0008-6223/

of both science and technology, a reliable and effective method to prepare FGQDs with tunable morphology and chemistry is highly desirable.

In this study, a strategy to tackle this dilemma and bridge the gap between concept and research is developed. Low-cost and commercially available fluorinated graphite (FGi) was first employed to produce FGQDs by a gradient fluorine-sacrificing strategy, which fundamentally avoids the toxic process to prepare FG by fluorinating graphene and the long-time hydrothermal-cutting treatment. The designed technologies and skills in our method also make it easy to gain finer and wider control over the chemical composition and size, which further allows us to gain a better insight into the fluorine effects on formation, luminescence, magnetism and cytotoxicity of FGQDs. The practically applicable experiment method, interesting achievements and useful research results presented here are expected to ignite more research flame into GQDs and other carbon materials, and promote the newly born FGQDs to find wider applications in various fields.

## 2. Experimental section

### 2.1. Raw materials

Fluorinated graphite (FGi, Grade II) was purchased from Shanghai CarFluor Ltd. and used as provided. KOH (≥82.0%), NaOH (≥96.0%) and other chemical reagents were purchased from Sinopharm Chemical Reagent Co., Ltd. and used without further purification. Ultra-pure water (>18 MΩ cm) was used throughout for preparation and washing.

### 2.2. Preparation of expanded FGi and hydroxyl-functionalized FG with gradient fluorine contents

To prepare expanded FGi (E-FGi), 100 mg dried FGi was blended uniformly with the mixed alkali (KOH—NaOH) powder in the following two designed recipes. For FG-1, the mass of the mixed alkali is about 318.7 mg; while for FG-2, the mass of the alkali is about 478.0 mg. Further increasing the mass ratio of alkali/FGi can also obtain similar products, yet the fluorine coverage becomes lower. So the reaction ratio was set as above to obtain FG sheets with higher fluorine and improved solubility in water. The mixture was then heated at 180 °C for 6 h in air and hydroxyl-functionalized E-FGi was obtained.

After cooling down to room temperature, the product was dispersed in ultra-pure water. After being sonicated for 2 h, single- or few-layered hydroxyl-functionalized FG sheets were finally obtained.

### 2.3. Preparation of FGQDs with tunable fluorine coverages and sizes

100 mg obtained FG samples was first dissolved into 10 mL concentrated $H_2SO_4$ and 3 mL ultra-pure water, and then the mixture was sonicated for 1.5 h to achieve a homogeneous dispersion. After another 10 mL concentrated $H_2SO_4$ and 60 mL $HNO_3$ were added, the mixture was sonicated for 3 h, followed being heated at 70 °C for 24 h. After cooling down to room temperature, 200 mL ultra-pure water was added and the pH of the solution was tuned neutral. Upon vacuum filtration (0.22 μm filter), FGQDs were finally obtained and collected by dialysis (molecular weight: 500 Da). Compared with reported work of preparing FGQDs [24], our method by using FGi as the raw material completely avoids the complex process to prepare FG with toxic and violent gases (such as $F_2$ or $XeF_2$). And compared with our previous work [25], this newly developed method can not only be realized in low temperature (the highest temperature is 120 °C, while the lowest temperature is 70 °C.), but also fundamentally avoids tedious long-time sonication and following high-temperature hydrothermal treatment, all of which make our method much more cost-effective and readily processible.

Samples FG-1 and FG-2 were treated under the same reaction conditions. To investigate the influence of temperature on FGQDs, sample FG-2 was reacted at 70 °C, 80 °C, 100 °C and 120 °C. And to evaluate the fluorine effects, GQDs was also prepared by using reduced graphene oxide under similar reaction conditions. Based on the reaction reagents and temperature, the products were abbreviated as FGQDs-1-70, FGQDs-2-70, FGQDs-2-80, FGQDs-2-100 and FGQDs-2-120.

### 2.4. Cellular viability

For 3-(4,5-dimethylthiazol-2-yl)-2,5-diphenyltetrazolium bromide (MTT) assay, Hela cells were employed to evaluate the biocompatibility of the as-prepared dried FGQDs powder. To calibrate the cellular survival rate, blank and control groups were set. In the blank group, only culture media was added; while in the control group, cells and culture media without samples were added. The measured optical density (OD) values of the blank, control, and experimental groups were coded as $OD_{bla}$, $OD_{con}$, and $OD_{exp}$, respectively. Finally, the cellular survival rate was calculated by the following equation:

$$\text{Survival Rate} = \frac{OD_{exp} - OD_{bla}}{OD_{con} - OD_{bla}} \times 100\%$$

The results were expressed as the mean ± SD (standard deviation).

### 2.5. Characterization and measurement

The chemical composition of the prepared samples was investigated by IFS 66 V/S Fourier transformation infrared (FTIR) spectrometer (Bruker, Germany), and X-ray photoelectron spectroscopy (XPS, EscaLab 250Xi) using a monochromated Al-Kα irradiation. The morphology of samples was observed by transmission electron microscopy (TEM) and high-resolution transmission electron microscopy (HRTEM, FEI Tecnai F30, operated at 300 kV), respectively. The photoluminescence excitation (PLE) and emission spectra were recorded on a FLS-920T fluorescence spectrophotometer equipped with a 450 W Xe light source and double excitation monochromators.

## 3. Results and discussion

It is suggested that two prerequisites guarantee the successful realization of exfoliating and modifying FGi in one step: one is that the high electronegativity gap between carbon and fluorine (4.0 for fluorine and 2.55 for carbon on the Pauling scale [26]) makes the carbon atom on FGi more positive, providing the possibility for nucleophilic hydroxyl to attack carbon and then substitute fluorine; the other is that the pre-designed nucleophilic reagents can provide mobile hydroxyl ions at a temperature much lower than the decomposition temperature of C—O and C—F, ensuring both the functionalization of oxygen and reservation of fluorine. Besides functionalization of FGi with hydroxyl to improve its solubility in water, after cooling down to room temperature the molten salts that have intercalated between FGi layers recrystallize and their volume expand, which further increases the interlayer space and finally facilitates the exfoliation. TEM images in Fig. 1 a, b clearly reflect the effective exfoliation and modification processes, both of which reveal that large, transparent and corrugated FG sheets with

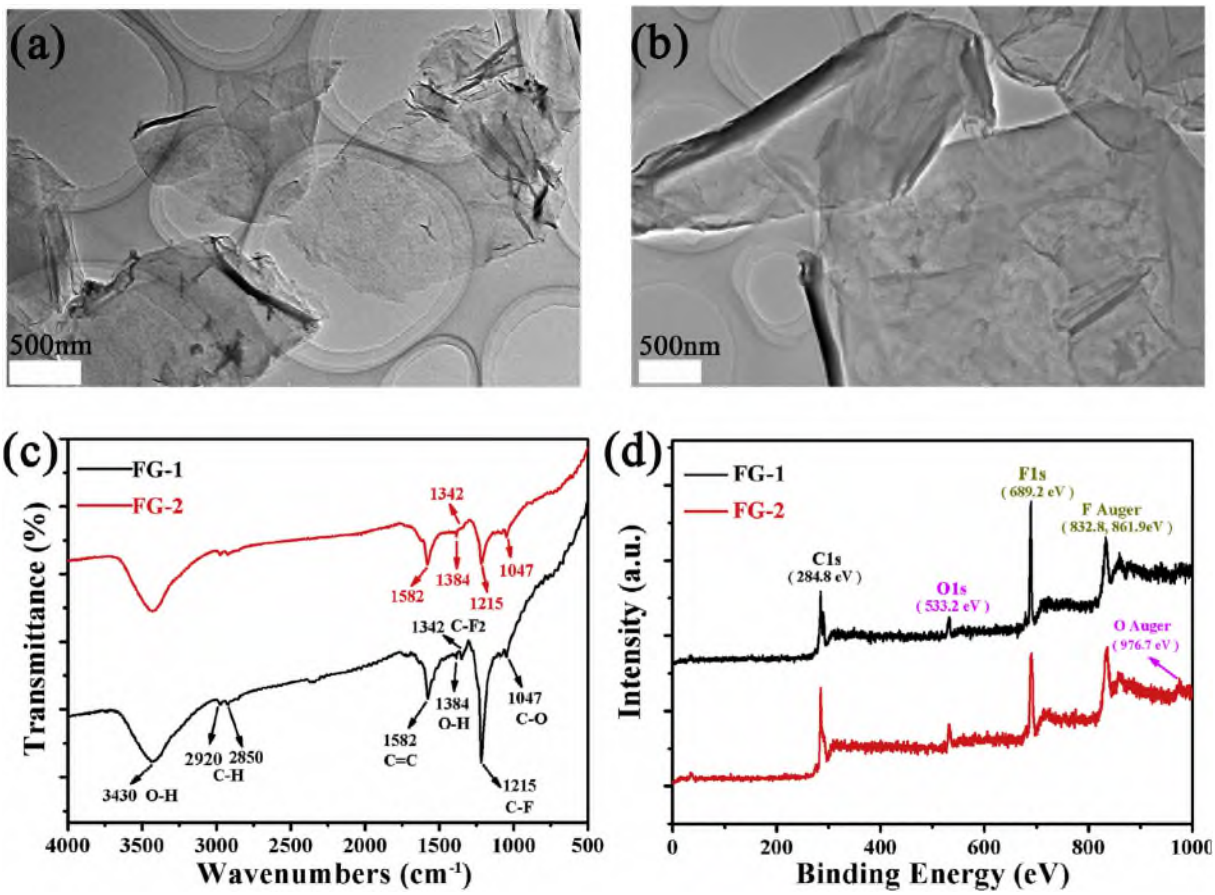


**Fig. 1.** TEM images of (a) FG-1 and (b) FG-2; (c) FTIR spectra and (d) full survey XPS spectra of FG-1 and FG-2. The chemical components and functional groups of the FG samples are labeled in the spectra. (A colour version of this figure can be viewed online.)

few layers are readily obtained. Then chemical composition analysis was carried out to investigate whether fluorine retains and hydroxyl invades as our initial design. FTIR spectra in Fig. 1c show that C—F bonds in the forms of covalent C—F (located at 1215 $cm^{-1}$) and $-CF_2$ (located at 1342 $cm^{-1}$) bonds robustly maintain on FG, and oxygen-containing groups in the forms of C—O (1047 $cm^{-1}$) and C—OH (1384, 3430 $cm^{-1}$) are successfully introduced onto FG [27]. This is also supported by XPS survey spectra imparted in Fig. 1d, in which both oxygen and fluorine elements are detected on the two prepared FG sheets.

Meanwhile, XPS investigation also gives the element composition of the two kinds of FG sheets (for FG-1, the fluorine content is about 29.7%; while for FG-2, the fluorine content is about 20.2%), confirming the fact that fluorine coverage on FG sheets can be predesigned by adjusting the ratio of alkali to FGi. These above data and discussions suggest that our method is more than a pretreatment of bulk FGi to prepare 0D FGQDs, it is also an effective method that realizes simultaneously modifying and exfoliating FGi to prepare 2D FG sheets. The successful introduction of hydroxyl into FG not only contributes to the exfoliation of FGi in water, but also greatly improves the solubility of FG, which can be dispersed in water and keep stable for days (Fig. S1 a-b). And it is just this dispersibility conversion from insoluble to soluble in water for FG that greatly facilitates the oxidization and cutting of FG in acid solution. Meanwhile, it is also observed that although following the way to prepare GQDs by adding mixed acid directly [27,29] can also obtain FGQDs, yet the yield is low. It is considered that even some fluorine atoms are removed from the structure, the FG sheets are still chemically inert to some degree. To improve this, a sonication-assisted pre-oxidized in acid before heating was developed (see the Experimental Section to prepare FGQDs) and it turns out working well.

A definitive quality identification of the prepared FGQDs was performed by TEM characterization to investigate their morphology. As depicted in Fig. 2a, FGQDs-1-70 with highly uniform size is successfully obtained, and a much closer look at the quantum dots in the magnified TEM image indicates the average lateral dimension of the sample is about 2.5 nm. Meanwhile, statistic size distribution in Fig. 2c indicates that the size of the FGQDs-1-70 mostly (about 80%) falls within the scope of 2 nm—3 nm. The crystallinity of the FGQDs-1-70 was investigated and revealed by HRTEM observation (the inset in Fig. 2b); the marked inter-planar distance of 0.21 nm agrees well with the (100) lattice spacing of graphene [30,31]. In contrast, FGQDs-2-70 prepared from FG with lower fluorine coverage obtained under the same conditions (heated at 70 °C) exhibits smaller sizes (Fig. 2d—f), and about 76% of the quantum dots are in the size range of 2 nm—3 nm, and about half are 2 nm. This interesting experimental discovery indicates that FG sheets with lower fluorine coverage might be softer to be oxidized and cut into quantum dots; under this assumption, the oxidizing acids will typically go after low-hanging fruit if they must choose one to cut, leading to the result of FG-2 to be more easily cut into smaller ones. Another amusing experimental phenomenon is that for FG-2, when the reaction temperature rises up to 120 °C, the average size of FGQDs-2-120 reaches up to 3.5 nm (See TEM images and statistic size distribution shown in Fig. 2g—i). Meanwhile, a

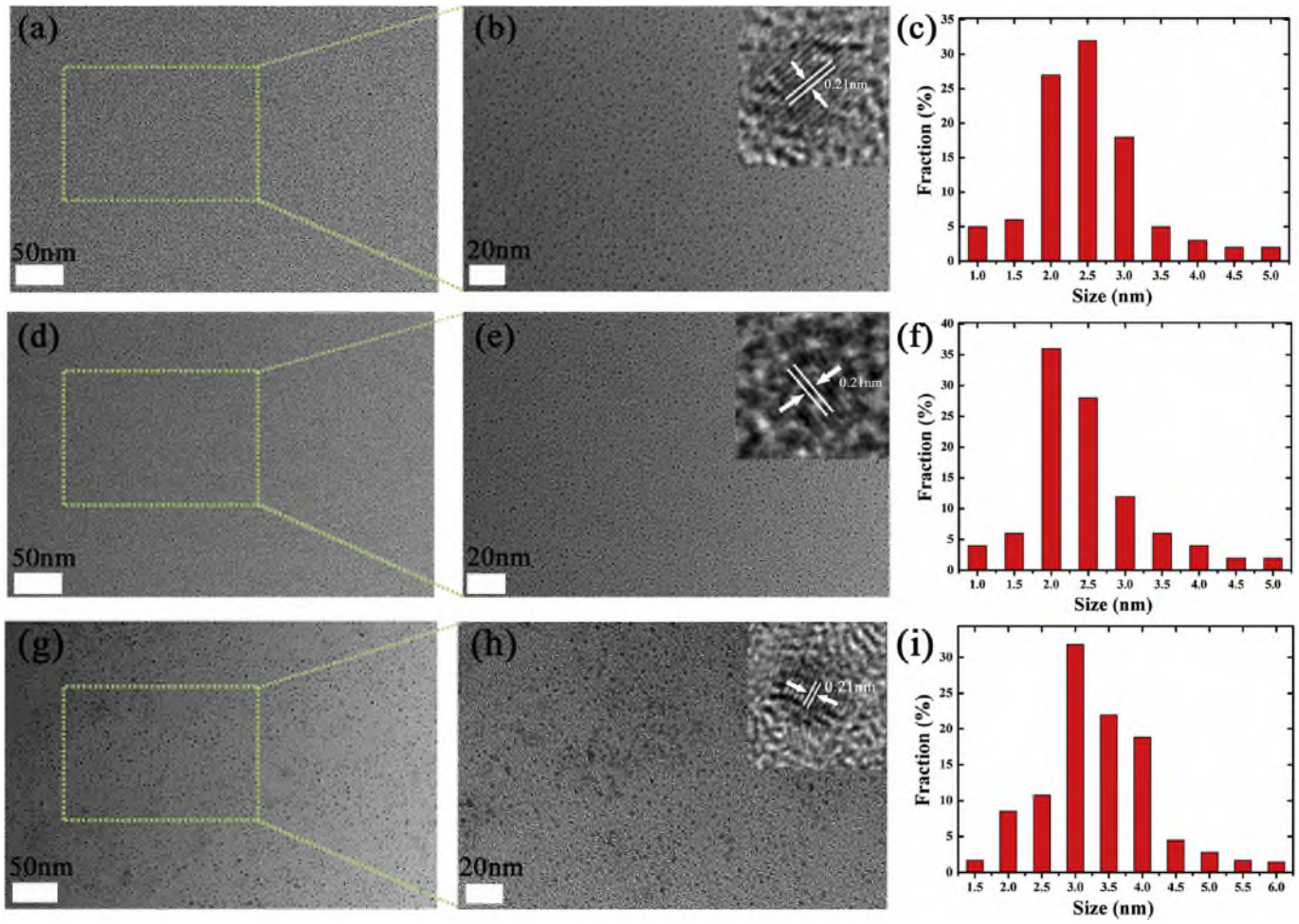


**Fig. 2.** TEM images of the obtained FGQDs samples: (a) A wide-field image of the obtained FGQDs-1-70; (b) A closer look at the size and shape of FGQDs-1-70; (c) Size distribution of FGQDs-1-70; Images of (d–f) and (g–i) show the corresponding experimental results of FGQDs-2-70 and FGQDs-2-120. (A colour version of this figure can be viewed online.)

more detailed inspection of the influence of temperature on the size of FGQDs (See TEM images and statistic size distribution in Figs. S2a–d) indicates that when the reaction temperature rises from 70, 80, 100–120 °C, the average lateral dimension of FGQDs-2 increases from about 2.0 nm (obtained at 70 and 80 °C), 3.0 nm (obtained at 100 °C) to 3.5 nm (obtained at 120 °C). If the heating process is compared to a sharp scissor in cutting FG into FGQDs, it is then concluded that when the scissor is hot-blooded, larger FGQDs can be tailored; if it is cold-blooded, smaller ones can be obtained. According to above experimental data and discussion, it is found this method is experimentally effective to synthesize FGQDs from commercially available bulk FGi, and more importantly, the sizes of FGQDs can be pre-designed by modulating the fluorine content or just by adjusting the heating temperature.

Morphology characterization and investigation clearly indicates that FGQDs with highly uniform size and tunable sizes can be readily realized, and then another key question that remains unexplored is whether fluorine atoms are still reserved after the cutting process and then how many of them are remaining on FGQDs. To address these issues, detailed chemical analyses of the samples are displayed in Fig. 3a–f. FTIR spectra in Fig. 3a clearly show that for the three samples, robust C–F bonds in the forms of covalent C–F (located at 1215 $cm^{-1}$) and $-CF_2$ (located at 1342 $cm^{-1}$) stably remain on the small scaffold of FGQDs [23]. Moreover, it is also observed that different from FG-1 and FG-2 that only contain C–O single bonds on FG sheets, a new absorption peak characteristic of C=O bonds (located at 1727 $cm^{-1}$) [27] appears in the three FGQDs, implying that during the oxidation and cutting processes, the FGQDs are further oxidized. Meanwhile, the chemical changes of the samples are also reflected and confirmed by XPS investigation in Fig. 3b–f.

To present clearer element information of the samples, XPS measurements were carried out on these FGQDs. XPS survey spectra in Fig. 3b reveal that only carbon, oxygen and fluorine elements can be detected, indicating the high purity of the samples. The investigation on element content shows that for samples of FGQDs-2-70 and FGQDs-2-120, their fluorine contents (18.2% for the former and 17.8% for the latter, respectively) are lower than that of FGQDs-1-70 (24.0%) obtained from FG-1 with higher fluorine coverage; it is also observed that the oxygen contents of FGQDs obtained from FG2 increase with the elevation of the heating temperature, suggesting that under the same conditions higher temperature can induce further oxidation of FGQDs. The detailed elemental composition of the samples obtained from XPS analyses are supplied in Fig. S3. Meanwhile, the F1s spectra of FGQDs (Fig. 3c) located at about 689.0 eV, agree well with the three peaks in the XPS survey spectra (located at 689.0, 832.7 and 861.8 eV), both of which can be ascribed to a reflection of covalent C–F bonds on a carbon structure [32]. A more visualized composition and nature of the chemical bonds of the samples were investigated by

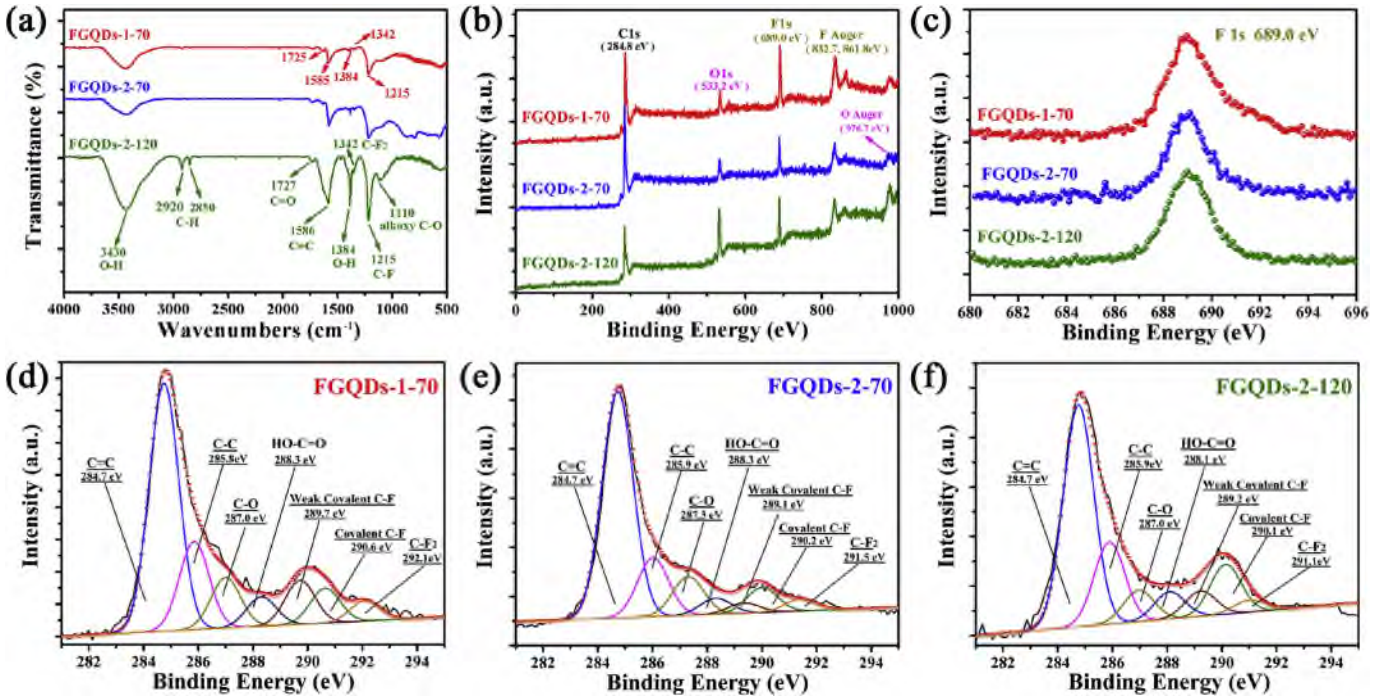


**Fig. 3.** Chemical composition analyses of the three samples. (a) FTIR spectra and (b) XPS survey spectra for FGQDs-1-70, FGQDs-2-70 and FGQDs-2-120. The chemical components and functional groups of the three FGQDs samples are labeled; (c) High resolution XPS spectra of F1s for the three samples; High resolution XPS spectra of C1s for (d) FGQDs-1-70, (e) FGQDs-2-70 and (f) FGQDs-2-120. (A colour version of this figure can be viewed online.)

high resolution XPS spectra in Fig. 3d–f. Three fitted peaks characteristic of weak covalent C–F bond (w-C–F, 289.3 eV), covalent C–F bond (290.0 eV) and $-CF_2$ bond (291.4 eV) can be readily found on the three samples; besides these, C–O groups in the forms of C–O (287.3 eV) and C=O (289.3 eV) also exist on the three FGQDs [31]. These above elemental analyses again demonstrate that C–F bonds remained on the structure of FGQDs and hydrophilic C–O groups are also successfully grafted onto the small scaffold of FGQDs. And these data further prove that our method is effective synthesize FGQDs, making it possible for FGQDs with tunable fluorine coverage to be obtained from commercially available bulk FGi in mild experimental conditions.

According to above data and discussions based on both morphological and elemental investigations, it is suggested that our method endows time-honored FGi with new glory; it is more than a traditional material with finite applications, but also a wonderful precursor to prepare 2D FG sheets and 0D FGQDs. And for the cutting process, the heating treatment acts as a scissor to cut larger 2D FG sheets into smaller 0D quantum dots. It is speculated that when the heating temperature is higher, the mixed acid is more active and corrosive, and thus its dash to FG sheets is considered more destructive. Accordingly, FG sheets tend to be cut into fragmentary ones with larger sizes and higher oxygen contents. When it is low, the oxidation and cutting process is less active and destructive, and this slowly gnawing process finally results in smaller ones with low oxygen contents. Therefore, it is observed in the experiment that smaller FGQDs with uniform sizes can be obtained under low temperature, while larger ones can be obtained under higher temperature. When it comes to the question that how the scissor works during the cutting process, it is proposed that during the oxidation process, epoxy groups tend to form a line on the lattice of FG and the cooperative alignment causes the rupture of the underlying C–C bonds, which may be similar to the preparation of GQDs from reduced graphene oxide or carbon nanotubes [27,33]. This proposed cutting process can also be supported by FTIR and XPS spectra of FGQDs in Fig. 3, in which significant carbonyl groups can be found. This is because these epoxy chains are energetically preferable to be further oxidized into epoxy pairs and then converted into more stable carbonyl groups even at room temperature [27,34]. According to above experimental results and discussion, the corresponding reaction processes to prepare FG and FGQDs are schematically summarized in Fig. 4.

Besides the aim of developing a practically applicable method to produce FGQDs with tunable size and controllable surface density, the fact that both deficient knowledge of FGQDs and the curiosity to uncover their mystery prompt us to explore the properties of FGQDs and find their potential applications. For FGQDs, one distinct property that other graphene or carbon quantum dots can't surpass is the stability due to strong C–F bond, which is stable up to 500 °C and thus they are more reliable in practical applications [28]. It is also found in our work that although the fluorine contents become lower after high-temperature processing and nearly complete removal of fluorine occurs after 500 °C, some stable C–F bonds of FGQDs can survive after high temperature (see XPS survey spectra of FGQDs-1-70 after being treated under 200 °C, 300 °C, 400 °C and 500 °C shown in Fig. S4). And among many of the exotic properties of GQDs, the optical performance is most alluring and it is also the fundamental one that determines its potential integration into optoelectronic, photo-catalyst, solar cells, light-emitting diodes and biological applications. Thus a systematic investigation on the PL performance is carried out on the obtained FGQDs and the corresponding results are displayed in Fig. 5 and Fig. S6. It is observed although FGQDs-1-70 and FGQDs-2-70 possess different sizes and element densities, they exhibit similar PL behavior; namely, both of them present a strong emission peak at about 430 nm when excited under 320 nm wavelength, and the PLE spectra of the two samples under the monitors of 431 nm and 430 nm show strong peaks around 320 nm, indicating that the small difference in size

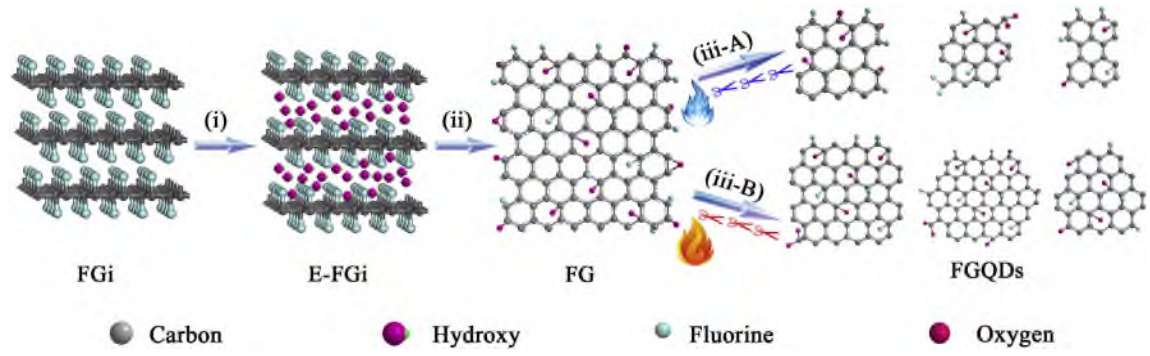


**Fig. 4.** Molecular models of fabrication processes for FGQDs: (i) Intercalation of molten alkali into pristine FGi to obtain E-FGi; (ii) Substitution and exfoliation processes; (iii-A) Lower temperature cutting to prepare FGQDs with smaller sizes; (iii-B) Higher temperature cutting to prepare FGQDs with larger sizes. For clarity, hydrogen atoms on graphene sheets and cations of the molten alkali in the reaction process are not shown. (A colour version of this figure can be viewed online.)

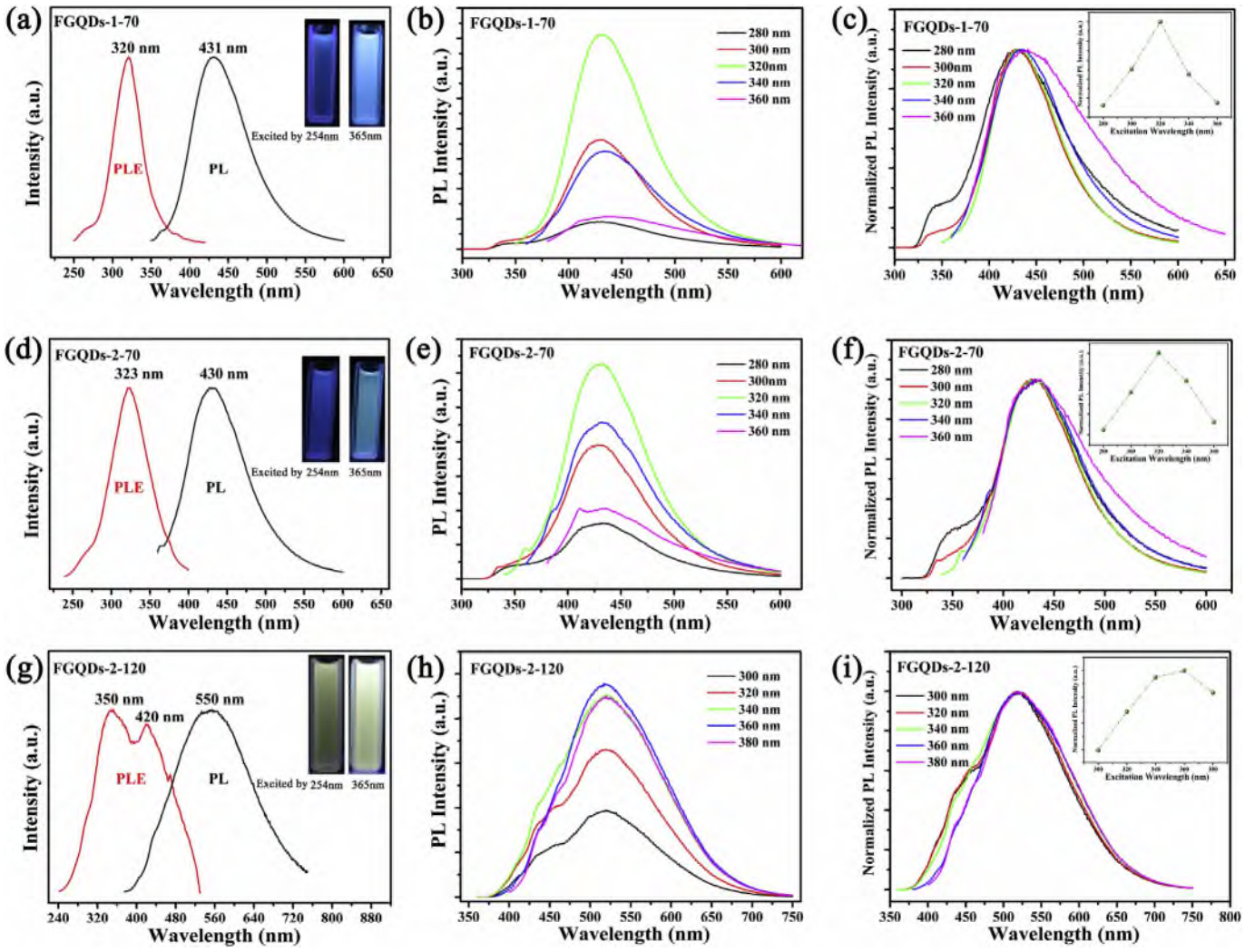


**Fig. 5.** Room temperature PL performance of the FGQDs samples dispersed in water: (a) PL and PL excitation (PLE) spectra of FGQDs-1-70, the insets show the corresponding luminescent images being excited by a UV beam of 254 and 365 nm, respectively; (b) PL spectra of FGQDs-1-70 at excitation wavelengths varying from 280 to 360 nm; (c) Normalized PL spectra of FGQDs-1-70 at different excitation wavelengths, the inset shows the corresponding variation of PL intensity at different excitation wavelengths; Data of (d–f) and (g–i) show the corresponding experimental results of sample FGQDs-2-70 and FGQDs-2-120, respectively. (A colour version of this figure can be viewed online.)

distribution and surface state between the two samples don't cast profound consequence on their PL behavior. On the other hand, a detailed comparison made between FGQDs-2 samples (Fig. 5 d, g and Fig. S6 a, d) clearly reveals that, with increasing the size the PL emission peak red-shifts from 430 nm (for FGQDs-2-70), 527 nm (for FGQDs-2-80), 545 nm (for FGQDs-2-100) to 550 nm (for FGQDs-2-120), indicating size effects gradually gain weight on the PL emission behavior of the samples. Also, it is noticed that

compared to FGQDs-1-70 and FGQDs-2-70, from sample of FGQDs-2-80, the PLE peaks of FGQDs-2 split into a predominant one at around 350 nm and a shoulder at around 400 nm. The PL performance of GQDs can be affected by the surface chemistry of foreign atoms or groups that induce electron transition from antibonding to nonbonding orbitals, and can also be influenced by size changes in the $sp^2$ domains [35–38]. For FGQDs, oxygen and fluorine atoms are co-doped in the structure, resulting in $sp^3$ hybrid carbon; besides, HRTEM investigation (Fig. 2) reveals that $sp^2$ domains also exist on the carbon structure of FGQDs. These data suggest that for FGQDs besides the intrinsic state emission (electron-hole recombination or quantum size effect/zigzag effect), defect state emission (surface defects) could also find a place in the luminescence behavior [8], which accounts for the split peak and the broadening peak width. This hypothesis well explains the PL performance of the samples, and is supported by the experimental data (see TEM and size distribution research in Fig. 2 and Fig. S2 as well as the chemical analyses of the samples in Fig. 3 and Fig. S5).

Besides the difference among them, all of the FGQDs also share a common yet extraordinary PL behavior: all FGQDs exhibit excitation-independent PL behavior. As can be observed in Fig. 5 b, e, h and Fig. S6 b, e, only the PL intensity while not the central peak position varies with excitation wavelength, and a much clearer impression of this experiment results are collected in Fig. 5c, f and i. This is a characteristic that can rarely be found in carbon-based fluorescent materials without surface-passivation, whose PL peaks often shift to longer wavelengths as the bathochromic shift of excitation wavelength is applied. Through literature research, it was found that this excitation-independent PL behavior has been reported in GQDs whose surfaces or edges are passivated by high temperature, or functionalized with hydrazide groups [39–41]. And in our case, it is observed in FTIR and XPS (see Fig. 3) investigations that abundant oxygen groups exist on the structure of FGQDs besides fluorine atoms, and contents of the functional groups are different in our samples, yet they share the similar excitation-independent behavior. So the surface passivation effect is not the predominant reason for the excitation-independent behavior of our samples. On the other hand, previous work pointed out that electronic properties and mechanisms involved in quantum-confined PL can induce excitation-independent behavior [37], and polydispersity of GQDs could also affect the PL spectra and cause excitation-dependent PL behavior [18], indicating that by carefully synthesizing GQDs with good size uniformity one can obtain GQDs exhibiting excitation-independent PL behavior. As have been studied in TEM investigation, every kind of FGQDs obtained by our method possesses relatively high uniform size and the majority of them exhibit similar sizes and structure. It is reasonable to speculate that the good size uniformity of FGQDs guarantees the extraordinary PL performance.

Another special property that makes FGQDs outstanding from other common graphene or carbon based quantum dots is their unique power to easily handle the provocation of pH on their own without any passivation, which previously could only be obtained in GQDs after being passivated by polymers [42]. PL emission intensity of GQDs without passivation often depends mostly on the pH of the solutions, which often quenches under acidic conditions. However, once powerful changes of pH can no longer greatly affect the PL emission intensity of FGQDs (Fig. 6), and robust luminescence can be readily obtained under different acid or base conditions without any after-treatment. Meanwhile, it is also observed that for these three samples, the more fluorine atoms they contain the less they are affected by change of pH. A close comparison between FGQDs-1 and FGQDs-2 reveals that a much smaller PL intensity deviation to the average value (the dash dot line in Fig. 6) occurs for FGQDs with higher fluorine coverage under different pH. It is no wonder that for FGQDs, this property does exist and fluorine atoms play the key role in the effective resistance of pH changes. Yet then the question is how fluorine atoms play the role?

The mechanism previously developed to explain the effects of pH mostly considers that a protonation and de-protonation process between the zigzag sites and hydrogen ion can affect the PL behavior of GQDs by changing the pH conditions [27], and that passivation of GQDs by removal of functional groups or decoration with polymers can also degrade the influence of pH changes [12]. On the other hand, according to classical Linus Carl Pauling theory on the electronegativity of element, fluorine atom enjoys the highest electronegativity value (4.0 on the Pauling scale) [26]. Thus the high electronegativity difference between fluorine and carbon (2.55 on the Pauling scale) makes it easy for the charge of carbon atoms on FGQDs to transfer onto fluorine atoms, and accordingly carbon atoms on the scaffold exhibit more positive charge. These positive carbon atoms on the small FGQDs not only greatly influence the charge distribution of FGQDs, but also effectively avoid or degrade the protonation process in acid condition due to electrostatic repulsion. And this further prevents the transition of carbene state on FGQDs, which in turn and finally leads to stable emission regardless of pH change [27]. On the other hand, it is also noticed that fluorine atoms can also dramatically affect the surface energy of FGQDs like other fluorine-contained carbon materials [43,44], and this effect also makes it possible for fluorine atoms on FGQDs play the role of passivation like polymers. Either the changes of charge distribution or surface energy of FGQDs, or both of them could cooperatively guarantee the stable emission of FGQDs regardless of the varying environmental conditions. It is believed that this pH-independent behavior of FGQDs could promote FGQDs to find applications that require stable emission under rigorous conditions while no other modification or passivation is involved.

The fine control over the chemical and structure of FGQDs also allows us to experimentally investigate the paramagnetism properties. As shown in Fig. 7, $M_S$ can be obtained by fitting the corresponding *M(H/T)* curves and clearly, fluorine atoms at a relatively low concentration can produce surprising enhancement of paramagnetism, which is about 5 times higher than GQDs without fluorine. Moreover, it is observed that FGQDs with different sizes and similar fluorine contents (for FGQDs-2-70 and FGQDs-2-120) possess close $M_S$ value, and for FGQDs that possess similar size and different fluorine contents (for FGQDs-1-70 and FGQDs-2-70), the higher fluorine contents the higher paramagnetism can be obtained. These data obviously reflect that it is the fluorine coverage rather than the size or oxygen that influences the paramagnetism improvement. And according to magnetism studies on graphene [18,45], it can be concluded that point defects induced by fluorine adatoms dominate the generation of localized spin magnetic moments on defective FGQDs. And from the aspect of structure, not all the fluorine atoms can contribute to the magnetism. The magnetic contribution can come only from cluster edges and would be determined by a particular configuration of fluorine atoms near the edges. These experimental findings firstly indicate that FGQDs not only enjoy highly fluorescent properties, but also exhibit noteworthy paramagnetism, which can be applied as a novel contrast agent for magnetic resonance imaging (MRI). And it is worthy noticing that compared to other MRI contrast agents, fluorinated ($^{19}F$) contrast agents are highly desirable due to the scarce distribution of fluorine in the human body, and thus the observed signals are robust and exhibit an excellent degree of specificity [46]. Therefore, our method provides a new and potentially valuable application of FGQDs in bio-imaging field, a single material possessing both fluorescence imaging and MRI.

The prerequisite for conducting bio-related research and exploring the potential bio-applications of FGQDs is to know their

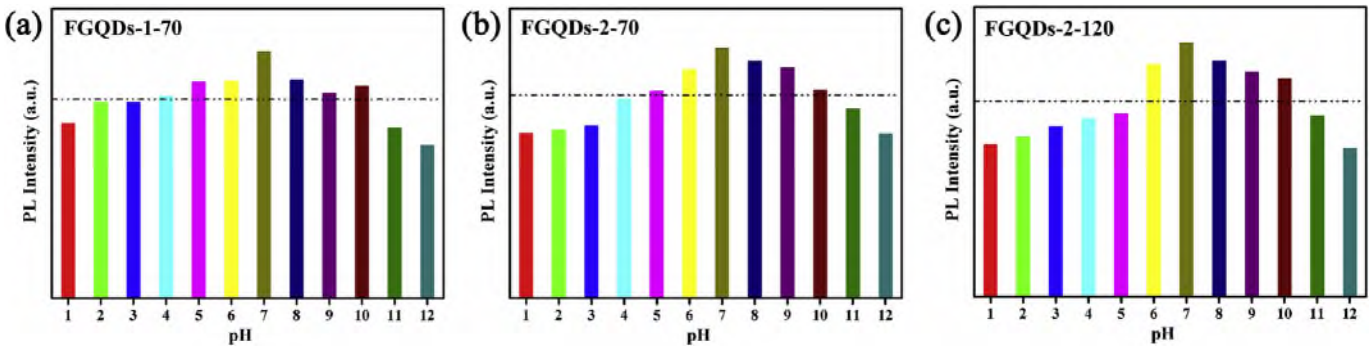


**Fig. 6.** pH effects on the PL behavior of sample (a) FGQDs-1-70, (b) FGQDs-2-70 and (c) FGQDs-2-120. (A colour version of this figure can be viewed online.)

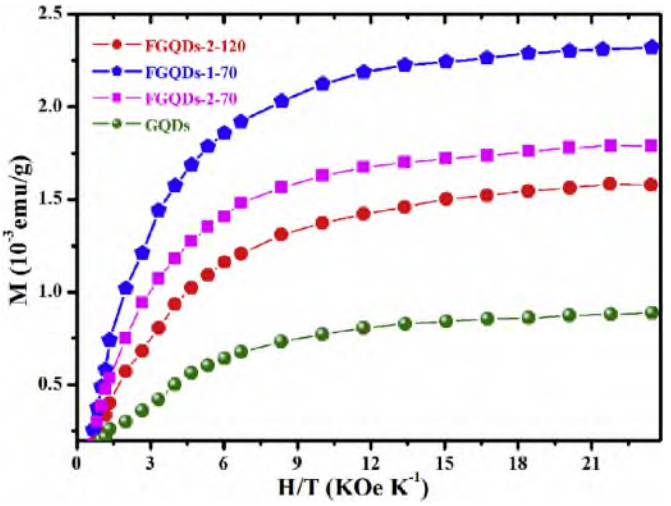


**Fig. 7.** Paramagnetism performance of FGQDs due to fluorine effects. (A colour version of this figure can be viewed online.)

toxicity effects on cells, so cell viability of Hela cells after being exposed to the three obtained FGQDs was evaluated and the corresponding results were summarized in Fig. 8. It is observed that all

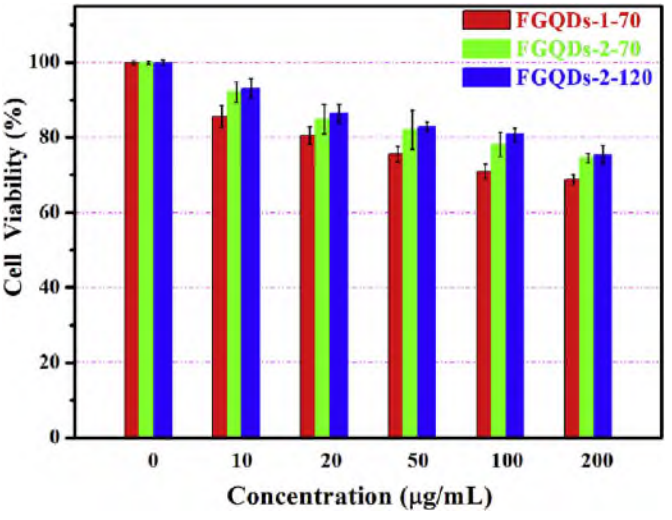


**Fig. 8.** Cell viability of Hela cells derived from the MTT assay measurements after 24 h exposure of the cells to FGQDs of various concentrations. (A colour version of this figure can be viewed online.)

FGQDs with different size and fluorine content exhibit low toxicity to cells even at a high concentration of 200 μg/mL. For FGQDs possessing similar size and different fluorine contents (FGQDs-1-70 and FGQDs-2-70), the one with less fluorine coverage exhibits less inhibition of cells; for FGQDs possessing similar fluorine contents and different sizes (FGQDs-2-70 and FGQDs-2-120), they exhibit nearly the same cell viability. This indicates that surface states have more influence than size on the cell activity. Furthermore, it is also concluded from these experiment data that for all the FGQDs, the cell viability obviously degrades with increasing the concentration of FGQDs. This unconventional behavior indicates that fluorination of GQDs can greatly modify the chemical and superficial environment of FGQDs, and finally lead to more sensitive response of the cells to the concentration changes.

## 4. Conclusions

In conclusion, our investigations on FGQDs concerning morphology, chemistry, PL performance, magnetism and cytotoxicity indicate that high-quality FGQDs with tunable size and fluorine coverage can be readily obtained from commercialized FGi, and fluorine atoms have great influence on their performance. By an effective control over the pre-treatment of FGi, once chemically inert bulk FGi becomes active and can be readily exfoliated into few-layered FG sheets, and further tailored into FGQDs. Fluorine atoms make FGQDs containedly resist pH effects, display stable luminescence in both acid and alkali conditions. Moreover, noteworthy paramagnetism induced by fluorine atoms endows FGQDs with potential MRI properties, which fundamentally distinguishes themselves from GQDs. And cytotoxicity experiment reveals that FGQDs possess good biocompatibility, and it is the surface state rather than the size of the FGQDs that have more influence on the cell viability. In a word, considering the mild reaction conditions, operational simplicity, effective tunability of the method, and the outstanding and novel properties of the FGQDs samples, this work will provide enlightening insights into chemical functionalization and preparation of GQDs, and promote the practical applications of FGQDs in novel fields.

## Acknowledgements

The authors thank Prof. Yuhua Wang, Prof. Desheng Xue and Daqaing Gao in Lanzhou University for PL and magnetism analyses. We also thank the financial support from the National Natural Science Foundation of China (Grant Nos. 51375474 and 51675514), the promotive research fund for young and middle-aged scientists of Shandong Province (ZR2016EMB04), Project of Shandong Province Higher Educational Science and Technology Program (J16LA03) and Doctoral Start-Up Scientific Research Foundation

(BSQD20150114) and Technology Program (xkj201602) of Qufu Normal University. Z. Wang also thanks the support from CAS Pioneer Hundred Talents Program.

## Appendix A. Supplementary data

Supplementary data related to this article can be found at http://dx.doi.org/10.1016/j.carbon.2016.10.091.

## References

[1] K.A. Ritter, J.W. Lyding, The influence of edge structure on the electronic properties of graphene quantum dots and nanoribbons, Nat. Mater 8 (2009) 235–242.
[2] J. Ge, M. Lan, B. Zhou, W. Liu, L. Guo, H. Wang, et al., A graphene quantum dot photodynamic therapy agent with high singlet oxygen generation, Nat. Commun. 5 (2014) 4596–4603.
[3] E. Hwang, S. Seo, S. Bak, H. Lee, M. Min, H. Lee, et al., An electrolyte-free flexible electrochromic device using electrostatically strong graphene quantum dot–viologen nanocomposites, Adv. Mater 26 (30) (2014) 5129–5136.
[4] Z.Z. Zhang, K. Chang, Tuning of energy levels and optical properties of graphene quantum dots, Phys. Rev. B 77 (2008) 235411.
[5] F. Libisch, C. Stampfer, J. Burgdörfer, Graphene quantum dots: beyond a dirac billiard, Phys. Rev. B 79 (2009) 115423.
[6] P. Hewageegana, V. Apalkov, Electron localization in graphene quantum dots, Phys. Rev. B 77 (2008) 245426.
[7] X. Geng, L. Niu, Z. Xing, R. Song, G. Liu, M. Sun, et al., Aqueous-processable noncovalent chemically converted graphene–quantum dot composites for flexible and transparent optoelectronic films, Adv. Mater 22 (30) (2010) 638–642.
[8] Z. Zhang, J. Zhang, N. Chen, L. Qu, Graphene quantum dots: an emerging material for energy-related applications and beyond, Energy Environ. Sci. 5 (10) (2012) 8869–8890.
[9] X. Zhou, Y. Zhang, C. Wang, X. Wu, Y. Yang, B. Zheng, et al., Photo-fenton reaction of graphene oxide: a new strategy to prepare graphene quantum dots for DNA cleavage, ACS Nano 6 (8) (2012) 6592–6599.
[10] M. Hassan, E.K. Haque, R. Reddy, A.I. Minett, J. Chen, V.G. Gomes, Edge-enriched graphene quantum dots for enhanced photo-luminescence and supercapacitance, Nanoscale 6 (20) (2014) 11988–11994.
[11] L. Tang, R. Ji, X. Cao, J. Lin, H. Jiang, X. Li, et al., Deep Ultraviolet photoluminescence of water-soluble self-passivated graphene quantum dots, ACS Nano 6 (6) (2012) 5102–5110.
[12] Q. Xue, H. Huang, L. Wang, Z. Chen, M. Wu, Z. Li, D. Pan, Nearly monodisperse graphene quantum dots fabricated by amine-assisted cutting and ultrafiltration, Nanoscale 5 (24) (2013) 12098–12103.
[13] Y. Li, Y. Zhao, H. Cheng, Y. Hu, G. Shi, L. Dai, L. Qu, Nitrogen-doped graphene quantum dots with oxygen-rich functional groups, J. Am. Chem. Soc. 134 (1) (2012) 15–18.
[14] F. Karlický, K.K.R. Datta, M. Otyepka, R. Zbořil, Halogenated graphenes: rapidly growing family of graphene derivatives, ACS Nano 7 (8) (2013) 6434–6464.
[15] Z. Wang, J. Wang, Z. Li, P. Gong, X. Liu, L. Zhang, et al., Synthesis of fluorinated graphene with tunable degree of fluorination, Carbon 50 (15) (2012) 5403–5410.
[16] K.J. Jeon, E. Pollak, L. Moreschini, A. Bostwick, C.M. Park, R. Mendelsberg, et al., Fluorographene: a wide bandgap semiconductor with ultraviolet luminescence, ACS Nano 5 (2) (2011) 1042–1046.
[17] P. Gong, J. Wang, W. Sun, D. Wu, Z. Wang, Z. Fan, et al., Tunable photoluminescence and spectrum split fromfluorinated to hydroxylated graphene, Nanoscale 6 (6) (2014) 3316–3324.
[18] Q. Feng, N. Tang, F. Liu, Q. Cao, W. Zheng, W. Ren, et al., Obtaining high localized spin magnetic moments by fluorination of reduced graphene oxide, ACS Nano 7 (8) (2013) 6729–6734.
[19] X. Hong, S.H. Cheng, C. Herding, J. Zhu, Colossal negative magnetoresistance in dilute fluorinated graphene, Phys. Rev. B 83 (2011) 085410.
[20] Y. Yang, G. Lu, Y. Li, Z. Liu, X. Huang, One-step preparation of fluorographene: a highly efficient, lowcost, and large-scale approach of exfoliating fluorographite, ACS Appl. Mater Interfaces 5 (24) (2013) 13478–13483.
[21] P. Meduri, H. Chen, J. Xiao, J.J. Martinez, T. Carlson, J.G. Zhang, et al., Tunable electrochemical properties of fluorinated graphene, J. Mater Chem. A 1 (27) (2013) 7866–7869.
[22] R. Romero-Aburto, T.N. Narayanan, Y. Nagaoka, T. Hasumura, T. Mitcham, M.T. Fukuda, et al., Fluorinated graphene oxide; a new multimodal material for biological applications, Adv. Mater 25 (39) (2013) 5632–5637.
[23] Y. Wang, W.C. Lee, K.K. Manga, P.K. Ang, J. Lu, Y.P. Liu, et al., Fluorinated graphene for promoting neuro-induction of stem cells, Adv. Mater 24 (31) (2012) 4285–4290.
[24] Q. Feng, Q. Cao, M. Li, F. Liu, N. Tang, Y. Du, Synthesis and photoluminescence of fluorinated graphene quantum dots, Appl. Phys. Lett. 102 (2013) 013111.
[25] P.W. Gong, Z.G. Yang, W. Hong, Z.F. Wang, K.M. Hou, J.Q. Wang, et al., To lose is to gain: effective synthesis of water-soluble graphene fluoroxide quantum dots by sacrificing certain fluorine atoms from exfoliated fluorinated graphene, Carbon 83 (2015) 152–161.
[26] D.R. Lide, CRC Handbook of Chemistry and Physics: a Readyreference Book of Chemical and Physical Data, 78th ed., CRC Press, 1997.
[27] D. Pan, J. Zhang, Z. Li, M. Wu, Hydrothermal route for cutting graphene sheets into blue-luminescent graphene quantum dots, Adv. Mater 22 (6) (2010) 734–738.
[28] X. Wang, Y.Y. Dai, J. Gao, J.Y. Huang, B.Y. Li, C. Fan, et al., High-Yield production of highly fluorinated graphene by direct heating fluorination of graphene-oxide, ACS Appl. Mater Interfaces 5 (2013) 8294–8299.
[29] J. Peng, W. Gao, B.K. Gupta, Z. Liu, R. Romero-Aburto, L. Ge, et al., Graphene quantum dots derived from carbon fibers, Nano Lett. 12 (2) (2012) 844–849.
[30] J. Zhou, C. Booker, R. Li, X. Zhou, T.K. Sham, X. Sun, et al., An electrochemical avenue to blue luminescent nanocrystals from multiwalled carbon nanotubes (MWCNTs), J. Am. Chem. Soc. 129 (4) (2007) 744–745.
[31] Y. Dong, H. Pang, H.B. Yang, C. Guo, J. Shao, Y. Chi, et al., Carbon-based dots co-doped with nitrogen and sulfur for high quantum yield and excitation-independent emission, Angew. Chem. Int. Ed. 52 (30) (2013) 7800–7804.
[32] Z. Wang, H. Zeng, L. Su, Graphene quantum dots: versatile photoluminescence for energy, biomedical, and environmental applications, J. Mater Chem. C 3 (2015) 1157–1165.
[33] Y. Dong, H. Pang, S. Ren, C. Chen, Y. Chi, T. Yu, Etching single-wall carbon nanotubes into green and yellow single-layer graphene quantum dots, Carbon 64 (2013) 245–251.
[34] Z. Li, W. Zhang, Y. Luo, J. Yang, J.G. Hou, How graphene is cut upon oxidation? J. Am. Chem. Soc. 131 (18) (2009) 6320–6321.
[35] T.F. Yeh, C.Y. Teng, L.C. Chen, S.J. Chen, H.S. Teng, Graphene oxide-based nanomaterials for efficient photoenergy conversion, J. Mater Chem. A 4 (6) (2016) 2014–2048.
[36] C.Y. Teng, T.F. Yeh, K.I. Lin, S.J. Chen, M. Yoshimura, H.S. Teng, Synthesis of graphene oxide dots for excitation-wavelength independent photoluminescence at high quantum yields, J. Mater Chem. C 3 (17) (2015) 4553–4562.
[37] T.F. Yeh, W.L. Huang, C.J. Chung, I.T. Chiang, L.C. Chen, H.Y. Chang, et al., Elucidating quantum confinement in graphene oxide dots based on excitation-wavelength-independent photoluminescence, J. Phys. Chem. Lett. 7 (11) (2016) 2087–2092.
[38] G.L. Li, H.L. Fu, X.J. Chen, P.W. Gong, G. Chen, L. Xia, et al., Facile and sensitive fluorescence sensing of alkaline phosphatase activity with photoluminescent carbon dots based on inner filter effect, Anal. Chem. 88 (5) (2016) 2720–2726.
[39] H. Yuan, X.H. Liu, L.M. Ma, P.W. Gong, Z.G. Yang, H.G. Wang, et al., High efficiency shear exfoliation for producing high-quality, few-layered $MoS_2$ nanosheets in a green ethanol/water system, RSC Adv. 6 (86) (2016) 82763–82773.
[40] G.L. Li, W.H. Kong, M. Zhao, S.M. Lu, P.W. Gong, et al., A fluorescence resonance energy transfer (FRET) based “Turn-On” nanofluorescence sensor using a nitrogen-doped carbon dot-hexagonal cobalt oxyhydroxide nanosheet architecture and application to α-glucosidase inhibitor screening, Biosens. Bioelectron. 79 (2016) 728–735.
[41] S. Zhuo, M. Shao, S.T. Lee, Upconversion and downconversion fluorescent graphene quantum dots: ultrasonic preparation and photocatalysis, ACS Nano 6 (2) (2012) 1059–1064.
[42] J. Shen, Y. Zhu, X. Yang, C. Li, Graphene quantum dots: emergent nanolights for bioimaging, sensors,catalysis and photovoltaic devices, Chem. Commun. 48 (31) (2012) 3686–3699.
[43] P.W. Gong, Z.F. Wang, Z. Li, Y.J. Mi, J. Sun, L. Niu, et al., Photochemical synthesis of fluorinated graphene via a simultaneous fluorination and reduction route, RSC Adv. 3 (18) (2013) 6327–6330.
[44] A. Mathkar, T.N. Narayanan, L.B. Alemany, P. Cox, P. Nguyen, G. Gao, et al., Synthesis of fluorinated graphene oxide and its amphiphobic properties, Part Part Syst. Charact. 30 (3) (2013) 266–272.
[45] R.R. Nair, M. Sepioni, I.L. Tsai, O. Lehtinen, J. Keinonen, A.V. Krasheninnikov, et al., Spin-half paramagnetism in graphene induced by point defects, Nat. Phys. 8 (2012) 199–202.
[46] S. Temme, F. Bönner, J. Schrader, U. Flögel, $^{19}F$ magnetic resonance imaging of endogenous macrophages in inflammation, Nanomed Nanobiotechnol 4 (3) (2012) 329–343.